4D flow MRI aortic cross-sectional pressure changes and their associations with flow patterns in health and aneurysm

Kevin Bouaou, Thomas Dietenbeck, Gilles Soulat, Ioannis Bargiotas, Sophia Houriez–Gombaud- Saintonge, Alain de Cesare, Umit Gencer, Alain Giron, Elena Jiménez, Emmanuel Messas, et al.

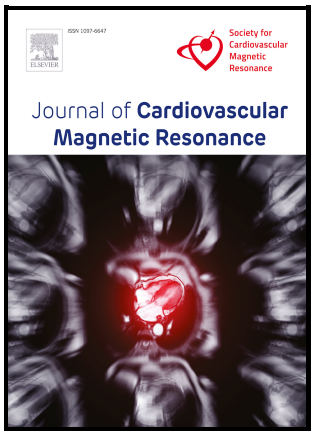

4D flow MRI aortic cross-sectional pressure changes and their associations with flow patterns in health and aneurysmBrief title: Pressure and flow in aortic aneurysm

Kevin Bouaou, Thomas Dietenbeck, Gilles Soulat, Ioannis Bargiotas, Sophia Houriez--Gombaud-Saintonge, Alain De Cesare, Umit Gencer, Alain Giron, Elena Jiménez, Emmanuel Messas, Didier Lucor, Emilie Bollache, Elie Mousseaux, Nadjia Kachenoura

PII: S1097-6647(24)01021-4

DOI: https://doi.org/10.1016/j.jocmr.2024.101030

Reference: JOCMR101030

To appear in: *Journal of Cardiovascular Magnetic Resonance*

Received date: 1 December 2023
Accepted date: 20 February 2024

Please cite this article as: Kevin Bouaou, Thomas Dietenbeck, Gilles Soulat, Ioannis Bargiotas, Sophia Houriez--Gombaud-Saintonge, Alain De Cesare, Umit Gencer, Alain Giron, Elena Jiménez, Emmanuel Messas, Didier Lucor, Emilie Bollache, Elie Mousseaux and Nadjia Kachenoura, 4D flow MRI aortic cross-sectional pressure changes and their associations with flow patterns in health and aneurysmBrief title: Pressure and flow in aortic aneurysm, *Journal of Cardiovascular Magnetic Resonance,* (2024) doi:https://doi.org/10.1016/j.jocmr.2024.101030

4D flow MRI aortic cross-sectional pressure changes and their associations with flow patterns in health and aneurysm

Kevin Bouaou[1], PhD, Thomas Dietenbeck[1], PhD, Gilles Soulat[2], MD, PhD, Ioannis Bargiotas[3], PhD, Sophia Houriez--Gombaud-Saintonge[1,4], PhD, Alain De Cesare[1], PhD, Umit Gencer[2], MS, Alain Giron[1], PhD, Elena Jiménez[1] MS, Emmanuel Messas[2], MD, PhD, Didier Lucor[5], PhD, Emilie Bollache[1], PhD, Elie Mousseaux[2], MD, PhD, Nadjia Kachenoura[1], PhD

[1]Sorbonne Université, INSERM, CNRS, Laboratoire d'Imagerie Biomédicale, Paris, France

[2]Hôpital Européen Georges Pompidou, INSERM 970, Paris, France

[3]CMLA, ENS Cachan, CNRS, Université Paris-Saclay, 94235 Cachan, France

[4]ESME Sudria Research Lab, Paris, France

[5]LIMSI, CNRS, Université Paris-Saclay, Orsay, France

Brief title: Pressure and flow in aortic aneurysm

Email-Addresses
KB: kevin.bouaou@gmail.com, TD: thomas.dietenbeck@sorbonne-universite.fr, GS: gilles.soulat@aphp.fr , IB: ioannisbargiotas@gmail.com, SHGS: sophia.houriezgombaudsaintonge@gmail.com, AdC: alain.decesare@lib.upmc.fr, UG: umit.gencer-ext@aphp.fr, AG: alain.giron@inserm.fr, EJ: elen.jimenez.sanchez@gmail.com, EMe: emmanuel.messas@aphp.fr, DL: didier.lucor@limsi.fr, EB: emilie.bollache@inserm.fr, EM: elie.mousseaux@aphp.fr, NK: nadjia.kachenoura@inserm.fr.

Acknowledgement and Disclosures

There are no relevant disclosures regarding the paper's contents

Corresponding Author. Nadjia Kachenoura, Laboratoire d'Imagerie Biomédicale, 15 rue de l'école de médecine, Paris, France ; Phone : +33144279116

Email: nadjia.kachenoura@inserm.fr

Abstract

Background

Ascending thoracic aortic aneurysm (ATAA) is a silent and threatening dilation of the ascending aorta (AscAo). Maximal aortic diameter which is currently used for ATAA patients management and surgery planning has been shown to inadequately characterize risk of dissection in a large proportion of patients. Our aim was to propose a comprehensive quantitative evaluation of aortic morphology and pressure-flow-wall associations from 4D flow MRI data in healthy aging and in patients with ATAA.

Methods

We studied 17 ATAA patients (64.7±14.3 years, 5 females) along with 17 age- and sex-matched healthy controls (59.7±13.3 years, 5 females) and 13 younger healthy subjects (33.5±11.1 years, 4 females). All subjects underwent an MRI exam including 4D flow and 3D anatomical images of the aorta. This latter dataset was used for aortic morphology measurements including AscAo maximal diameter (iD_{MAX}) and volume, indexed to body surface area. 4D flow MRI data were used to estimate: 1) cross-sectional local AscAo spatial (ΔP_S) and temporal (ΔP_T) pressure changes as well as the distance (ΔD_{PS}) and time duration (ΔT_{PT}) between local pressure peaks, 2) AscAo maximal wall shear stress (WSS_{MAX}) at peak systole, 3) AscAo flow vorticity amplitude (V_{MAX}), duration (V_{FWHM}) and eccentricity (V_{ECC}).

Results

Consistency of flow and pressure indices was demonstrated through their significant associations with AscAo iD_{MAX} (WSS_{MAX}: r=-0.49, p<0.001; V_{ECC}:r=-0.29, p=0.045; V_{FWHM}:r=0.48, p<0.001; ΔD_{PS}:r=0.37, p=0.010; ΔT_{PT}:r=-0.52, p<0.001) and indexed volume (WSS_{MAX}:r=-0.63, V_{ECC}:r=-0.51, V_{FWHM}:r=0.53, ΔD_{PS}:r=0.54, ΔT_{PT}:r=-0.63, p<0.001 for all). Intra-AscAo cross-sectional pressure

difference, ΔP_S, was significantly and positively associated with both V_{MAX} (r=0.55, p=0.002) and WSS_{MAX} (r=0.59, p<0.001) in the 30 healthy subjects (48.3±18.0 years). Associations remained significant after adjustment for iD_{MAX}, age and systolic blood pressure. Superimposition of ATAA patients to normal aging trends between ΔP_S and WSS_{MAX} as well as V_{MAX} allowed identifying patients with substantially high pressure differences concomitant with AscAo dilation.

Conclusion

Local variations in pressures within ascending aortic cross-sections derived from 4D flow MRI were associated with flow changes, as quantified by vorticity, and with stress exerted by blood on the aortic wall, as quantified by wall shear stress. Such flow-wall and pressure interactions might help for the identification of at-risk patients.

Keywords

4D flow MRI; ascending thoracic aortic aneurysms; aortic pressure; vorticity; wall shear stress; remodelling

Background

Ascending thoracic aortic aneurysm (ATAA) is an asymptomatic dilation of the ascending aorta (AscAo) that can ultimately lead to aortic dissection and consequently to an increased morbi-mortality. AscAo dilatation is frequently observed in specific diseases such as bicuspid aortic valve as well as Marfan or Turner syndromes, but also in the general population [1]. Clinical recommendations for the evaluation of risk of aortic rupture and prophylactic surgery planning are mainly based on the measurement of maximal aortic diameters from imaging data [2] such as echocardiography, computed tomography (CT) and MRI angiography. Such diameter measures are often performed on pre-selected

2D slices. An ATAA patient requires follow-up once maximal aortic diameter exceeds 42 mm and when such diameter exceeds 55 mm, the patient is referred to surgery. However, a patient may undergo aortic dissection despite an aortic diameter below surgical threshold[3]. Accordingly, new more sensitive and specific indices are urgently needed to precisely identify patients at risk of aortic rupture. Automated 3D segmentation methods have been proposed to extract morphological parameters such as aortic length, volume and curvature for all thoracic aorta regions from 3D MRI images [4,5] or CT [6] angiograms. In addition to such 3D aortic morphology, MRI can provide a functional evaluation of the aorta including quantitative analyses of aortic blood flow using 4D flow sequences. Several studies have highlighted the development of specific flow patterns in aortic dilatation [7,8]. Such flow patterns have been characterized using 4D flow MRI through various quantitative parameters [7,9], including : 1) wall shear stress (WSS) [10,11];; 2) vorticity patterns [5,12] 3) intra-arterial pressure changes through the aortic length which has demonstrated added value in valve stenosis or aortic coarctation [13]. Of note, to the best of our knowledge, pressure differences within aortic cross-sections, which can provide insight into how changes in geometry locally affect blood flow, have never been investigated. Such cross-sectional component can be of particular interest since aneurysm morphology may be variable exhibiting asymmetric or localized dilation.

Aorta has been described using the multiple abovementioned morphological and velocity-based quantitative parameters. However, the interaction between these various complementary parameters in health and aneurysmal disease remains underexplored. Thus, our objectives are: 1) to estimate aortic cross-sectional pressure differences as well as flow vorticity and WSS non-invasively in the AscAo using 4D flow MRI data; 2) to study the relationship between these flow parameters and aortic 3D-derived morphological parameters, namely maximal diameter and volume; 3) to investigate the

associations and interactions between velocity-derived features (pressure, WSS, vorticity). To achieve these objectives, we performed our analyses on: 1) patients with ascending aorta dilatation and a tricuspid aortic valve, 2) healthy volunteers matched for age, sex and blood pressure to the dilated patients, and 3) healthy and young volunteers providing normality for all aortic parameters. The abovementioned matching is crucial because age, sex and blood pressure are major confounding factors for the targeted aortic measurements.

Methods

Study population and data acquisition

We retrospectively studied 17 ATAA patients (64.7±14.3 years, 5 females) with a tricuspid aortic valve without severe stenosis, regurgitation or previous surgery. ATAA was defined by a maximal diameter over the ascending aorta ≥ 41 mm or ≥ 22 mm/m² when indexed to body surface area (BSA). We also studied 17 healthy subjects (59.7±13.3 years, 5 females) matched for age, sex and systolic blood pressures to the ATAA patients, as well as 13 younger and healthy individuals (33.5±11.1 years, 4 females) to derive representative "normal" quantitative measures and associations. MRI data of these healthy individuals are part of a local protocol focusing on the non-invasive evaluation of myocardial stiffness by ultrafast echo as compared to MRI (NCT02537041). Accordingly, the present ancillary work objectives are independent from the goals of the primary protocol. Approval from the local ethics committee and subjects informed consent were obtained.

MRI was performed on a 3T scanner (Mr750w GEM, GE Healthcare, Chicago, IL, USA) with a 32-channel cardiac phased-array coil, after injection of gadolinium-based contrast agent (0.1 to 0.2

mmol/kg). 4D flow data were acquired during free-breathing with retrospective ECG gating in a sagittal oblique volume encompassing the thoracic aorta, using the following scan parameters: echo time=1.7 ms, repetition time TR=4.3-4.4 ms, flip angle=15°, voxel size=1×1.48×2.38 mm^3, and velocity encoding=250 cm/s in all directions. Velocities were encoded in each direction with a balanced four-point scheme obtained every 4 TR. The number of views per segment was fixed to 2 and total acquisition duration was around 10 minutes. Datasets had an effective temporal resolution of 34.8 ms, and were reconstructed with 50 cardiac phases after using view sharing independent of heart rate. Brachial pressures were recorded simultaneously to MRI acquisitions using the SphygmoCor Xcel device (AtCor Medical, Australia), while immediately after, applanation tonometry of the right carotid artery was performed by an experienced operator (10 years) with the PulsePen device (DiaTecne, Milano, Italy). Applanation tonometry acquisitions were performed in a lying position and in a temperature controlled semi-dark room, to reproduce MRI exam conditions, resulting in central systolic (SBP) and diastolic (DBP) blood pressures.

Additionally, to assess morphology, all patients underwent a sagittal oblique volume acquisition encompassing the entire thoracic aorta using a 3D spoiled gradient recalled (SPGR) sequence with the following scan parameters: flip angle=24°, repetition time=3.1 ms, echo time=1.3 ms, voxel size=0.67×0.67×3.2mm^3.

Image pre-processing and aortic segmentation

The SPGR images were used for semi-automated 3D aortic segmentation through an explicit active contours algorithm implemented within the Mimosa software (LIB, Sorbonne University, Paris), which was previously shown to reproducibly quantify aortic morphology [4]. Such segmentation enabled the

quantitative measurement of AscAo maximal diameter (D_{MAX}) perpendicular to the centreline and volume (Vol_{AscAo}). AscAo maximal diameter and volume were then indexed to body surface area (iD_{MAX}, $iVol_{AscAo}$).

4D flow MRI data were corrected for phase offset and phase wrapping according to guidelines [7]. A time-averaged phase-contrast MR angiography (PC-MRA) was then derived from the 3 directional velocities weighted by the modulus images, when considering 5 time phases around the systolic peak, which was defined as the temporal phase with maximal velocity in the ascending aorta [13]. Finally, the same aforementioned segmentation algorithm [4] was applied to the resulting PC-MRA dataset to segment the thoracic aorta volume, define the aortic centreline and thus isolate aortic velocity fields.

In addition, for each subject, PC-MRA segmentation was used to further define 64 cross-sectional planes perpendicular to the aortic centreline from the most proximal level of the AscAo, to the celiac trunk bifurcation. AscAo segment was delimited by the brachiocephalic bifurcation (Figure 1) and comprised 5 to 11 cross-sectional planes, depending on individual AscAo length. Algorithms and user interface were implemented in Matlab (The Mathworks, Natick, MA, USA).

Quantitative indices of intra-aortic pressures

The 3D+t aortic pressure maps relative to the zero reference set at the most proximal level of the AscAo were obtained while applying pressure Poisson equations to the 4D flow MRI velocity fields delimited by the aortic segmentation of the PC-MRA dataset as previously described [14]. To capture the effects of changes in blood flow patterns on intra-aortic pressure distribution, several quantitative cross-sectional indices reflecting either spatial or temporal pressure variations were derived from the time-resolved relative pressure maps within the AscAo segment (Figure 1). Spatial pressure quantitative

indices included: 1) maximal pressure difference within each slice (magnitude between pressure extrema within such single cross-sectional location) for each time phase ($\Delta P_S(t)$), which was then averaged for all AscAo cross-sectional planes, to minimize the effect of noise (Figure 2), and its maximal value through time was named ΔP_S, (mmHg) ; 2) the distance between pressure extrema within each slice and for each time phase ($\Delta D_{PS}(t)$), which was then averaged for all AscAo cross-sectional planes and its maximal value through time was named ΔD_{PS} (mm). Finally, relative pressure time curve averaged across all AscAo cross-sectional planes was calculated and used to estimate the following pressure quantitative indices: 1) the difference in magnitude between systolic and diastolic relative pressure peaks (ΔP_T, mmHg); 2) the duration between these two peaks (ΔT_{PT}, ms).

Quantitative indices of vorticity

The λ2-method that was initially proposed by Jeong & Hussian [15] and validated quantitatively in several studies [12,16] was used for vortex identification in our segmented aortic 4D flow data. The following parameters were then estimated in each cross-sectional plane of the AscAo (Figure 1): 1) the peak vortex amplitude across the cardiac cycle (V_{MAX}) derived from the vorticity time curve, which was averaged over the whole AscAo segment for each time phase; 2) average vortex duration in the AscAo, which was defined as the full width at half maximum (V_{FWHM}, ms) of the aforementioned vorticity time curve. In addition, vortex eccentricity was estimated as the distance between the vortex centre and the aortic centreline indexed by local aortic diameter (V_{ECC}), where vortex centre was defined as the centre of mass of the largest cluster of pixels identifying a vortex.

Quantification of wall shear stress

WSS was calculated using the method previously described by Potters et al. [17], which minimizes

errors related to the estimation of the spatial variations of blood flow velocities at the aortic wall boundaries. Briefly, space rotation was performed to be able to locally define the vector normal to the aortic wall according to a single coordinate, namely z. This rotation was individually applied to each point of the aortic segmentation where WSS was calculated.

WSS was evaluated for all aortic segmentation points and at all cardiac cycle time-phases (Figure 1). Then spatial maxima of WSS were estimated at systolic peak for each plane of the AscAo segment, and were averaged resulting in maximal AscAo WSS (WSS_{MAX}).

Statistical analysis

Continuous variables were provided as mean ± standard deviation for each group, after testing for the normality of their distribution using the Shapiro-Wilk test. Linear regressions were used to study associations between AscAo 4D flow MRI-derived indices, namely relative pressure, WSS and vorticity as well as their associations with indices of AscAo morphology including maximal diameter and volume. For each linear regression, correlation coefficient and p value were provided and further adjustment for age and SBP, as well as iD_{MAX} when appropriate, was performed using a multivariate regression model. Statistical differences between groups were tested using the nonparametric Wilcoxon rank-sum test. All reported p-values were two-sided and statistical significance was indicated by a p-value < 0.05. Analyses were performed using Stata software (StataCorp, TX, USA).

Results

Figure 3 shows two examples of 3D blood flow velocity, relative pressure and WSS maps derived from 4D flow MRI of a young healthy subject and a patient with dilated ascending aorta along with time-

resolved velocity, WSS, vorticity and relative pressure curves in the ascending aorta averaged over young and elderly healthy subjects as well as ATAA patients. The 3D maps highlighted a drop in velocity magnitude, spatial pressure difference as well as WSS in the dilated AscAo, as compared to the AscAo of the healthy subject. In line with these qualitative observations in single cases, time-resolved curves illustrated that both physiological (aging) and to a greater extent pathological (ATAA) aortic dilatations were associated with: 1) a decrease in blood flow velocity magnitude, 2) a decrease in wall shear stress magnitude, 3) a decrease in vortex magnitude along with an increase in its duration, and 4) a decrease in relative pressure magnitude along with an earlier occurrence of its second peak.

Consistently with the illustrated trends, Table 1 summarizes patients and healthy subject characteristics along with MRI-derived quantitative AscAo morphological and hemodynamic measures. Four ATAA patients had mild aortic valve regurgitation (AR), 4 had moderate AR while the remaining 9 patients had no AR. According to our study design, there were no significant differences in age, SBP, DBP and body surface area between ATAA patients and their matched controls. SBP was slightly higher in the elderly controls as compared to the younger healthy controls. We found a physiological enlargement of the aorta with age, as revealed by the significant increase in AscAo maximal diameter and volume in the elderly controls as compared to the younger healthy controls. Such aortic enlargement was expectedly even more pronounced in ATAA patients.

Furthermore, while WSS was significantly lower in the elderly as compared to younger controls and even lower in ATAA patients, vortex duration was significantly higher in ATAA patients and lowest in healthy younger controls. Vortex amplitude has a decreasing trend between young and elderly controls and was significantly lower in ATAA patients as compared to elderly controls. Among pressure indices, duration between systolic and diastolic relative pressure peaks, ΔT_{PT}, was lower in

the elderly controls as compared to younger controls and even lower in the ATAA patients. The distance between relative pressure extrema within the AscAo was significantly higher in the ATAA patients as compared to their matched controls, as well as between elderly and younger controls.

Associations between ascending aorta hemodynamic and morphological indices

Associations between hemodynamic and both indexed or non-indexed AscAo maximal diameter and volume for the entire study group are summarized in Table 2. We found a significant and negative association between WSS_{MAX} and both AscAo diameter and volume. Vortex eccentricity in the ascending aorta (V_{ECC}) was negatively and significantly associated with AscAo diameter and volume. Vortex duration (V_{FWHM}) showed a significant increase with AscAo diameter, and volume. In addition, the distance between cross-sectional pressure extrema within the AscAo (ΔD_{PS}) was significantly and positively correlated with AscAo diameter, and volume. Finally, the duration between systolic and diastolic relative pressure peaks within the AscAo (ΔT_{PT}) decreased significantly with AscAo diameter, and volume. Most of these associations remained significant after adjustment for age and SBP (Table 2).

Associations between pressure and flow in normal aging

Table 3 summarizes associations of intra-aortic pressure indices with flow parameters such as vorticity and WSS in healthy subjects (30 subjects, 9 women, mean age: 48.3±18.0 years), revealing that when local spatio-temporal pressure differences increase there is an increase in WSS along with high magnitude but quickly vanishing vortex. Indeed, maximal cross-sectional spatial pressure difference within the AscAo (ΔP_S) was significantly and positively correlated with WSS_{MAX} (Figure 4A) and maximal vorticity magnitude V_{MAX} (Figure 4B), while it was significantly and negatively correlated

with vortex duration V_{FWHM}. Figure 5 illustrates examples of extreme values of ΔP_S along with the corresponding changes in ascending aorta velocity, WSS and vorticity throughout the cardiac cycle. Of note, associations with WSS_{MAX} and V_{MAX} were independent of age, SBP and AscAo indexed maximal diameter (p=0.03 and p=0.006, respectively). Furthermore, difference in magnitude between systolic and diastolic relative pressure peaks (ΔP_T) was significantly and positively correlated with WSS_{MAX}, while it was significantly and negatively correlated with vortex eccentricity V_{ECC}.

Associations between pressure and flow in aortic dilation

Figure 6 illustrates the abovementioned "normal" linear regressions of pressure with WSS and vorticity magnitude with further superimposition of patients with ATAA, revealing that, thanks to their remodelled dilated lumen, more than half of ATAA patients had low spatial intra-ascending aorta cross-sectional pressure differences, with similar magnitude as elderly subjects. However, one might highlight that some ATAA patients (6/17 patients) had elevated intra-aortic pressure differences despite their AscAo dilatation (5 of these 6 patients had a non-indexed AscAo maximal diameter >41 mm).

Discussion

Novel indices to quantify cross-sectional and temporal pressure changes within the ascending aorta from 4D flow MRI images were proposed and were shown to be mechanistically associated with aortic geometry, WSS as well as vortex amplitude, duration and eccentricity in health and aortic dilation.

Intra-aortic pressure gradients can be decomposed into: 1) longitudinal pressure gradient along the aorta, which measures pressure gradients through the aortic length. It is valuable for the assessment of the overall effect of geometrical changes, including pathological dilation or narrowing and even

physiological tapering [14,18,19], on pressure distribution. Such longitudinal pressure gradient can help evaluate the uniformity/non-uniformity as well as the severity of the geometrical changes. Indeed, several studies focused on intra-aortic pressure mapping from 4D flow MRI images either in patients or healthy volunteers [13,18,20,21], highlighting the ability of the resulting maps to capture both disease-related and subclinical changes in local pressure differences through the aortic length. Associations of such longitudinal changes with pressure wave reflection and LV remodelling in aging have also been reported [14]. 2) Transverse or cross-sectional pressure gradient focuses on pressure differences within aortic cross-sections providing insight into how a local change in geometry locally affects blood flow. Indeed, aortic curvature is shown to affect pressure patterns inducing higher pressures in the external part of the curved aortic segment [18], as is the case in the ascending aorta. Aortic cross-sectional pressure gradients can be particularly valuable in aneurysms with variable morphology exhibiting asymmetric or localized dilation. As such, regions of high- or low-pressure within the aneurysm can be assessed through such cross-sectional pressure gradient and potentially help identifying areas at risk of rupture or dissection.

4D flow MRI has been used in several recent studies in aging and in aortic diseases to individually estimate aortic stiffness [22,23], WSS [24,25], intra-aortic relative pressures along with their changes through the aortic length [13,14,18,19] as well as vorticity [5,26].. Aortic WSS has been widely documented in terms of methodological [27–30] and clinical [31–35] evaluations with a specific focus on patients with a bicuspid aortic valve-[31,33]. Fewer studies focused on vorticity per se with a very pioneering work from Kilner et al. [36], and few recent studies described and quantified blood flow vortical organization in the thoracic aorta of healthy subjects [5,12], as well as vanishing and altered patterns in patients, while using the λ2 method [12]. Of note, WSS and vorticity values obtained in our

population are in the same range as values provided in the abovementioned WSS [32,37,38] and vorticity [12] studies. One might highlight however that changes in flow patterns in the thoracic aorta have been widely described through the quantitative evaluation of backward flow from 2D phase contrast MRI [39] and more recently from 4D flow MRI [40]. Such backward flow, which starts during late systole and persists until late diastole, has been attributed to the local reversal of pressure gradients [41,42] inducing a local reversal in blood flow, captured by the velocity sign on either 2D or 4D phase contrast MRI images. Flow reversal patterns are mostly located in the curved segments of the aorta [40], which is in line with the higher convective relative pressures observed in the external part of such segments [18] and with cross-sectional changes in aortic pressure gradients found in our study.

In the present study, consistency of the comprehensive quantification of 3D anatomical and 4D flow images was evaluated through associations between cross-sectional pressure or flow parameters and morphological indices of the aorta. As such, we found a decrease in maximum WSS in dilation, which is in line with literature findings [32]. Besides, a reduction in the magnitude of the vortex as well as an increase in its duration were observed with increasing aortic size, in agreement with visual or quantitative findings in the literature [5,43]. Furthermore, our data revealed that vortices tended to be eccentric in normal-sized aortas and more centralized in dilated aortas. This result is consistent with observations in aging, since backward flow area in the ascending aorta is confined to its inner curvature in young subjects and tends to grow and appear in a larger proportion of the lumen in elderly subjects with larger aortic stiffness and dimensions [39]. Finally, we found that the duration between systolic and diastolic pressure peaks tends to be shorter in larger aortas. This is consistent with previous findings [14] and might be explained by the early return of wave reflections in larger and stiffer aortas.

Regarding flow and pressure associations in healthy aging, we found a positive association of WSS

and vortex magnitudes with spatial and temporal cross-sectional pressure differences. These associations might be explained by the fact that blood flow orientation and velocity are locally governed by pressure gradients. Indeed, a locally important pressure difference seems to be associated to a high magnitude vortex and high WSS exerted on the inner aortic wall. These preliminary associations highlight that spatio-temporal knowledge on intra-aortic cross-sectional pressure distribution could give indications on local flow pattern changes and their interaction with the aortic wall.

Finally, superimposition of ATAA patients data to "normal" trends associating pressure with flow indices revealed that more than half of the dilated patients had the same distribution as elderly subjects. These patients seem to present regularized and pseudo-normalized pressure gradients, vorticity and WSS through the augmentation of their ascending aorta size. However, one third of the patients had elevated intra-aortic pressure differences despite AscAo dilatation. These latter patients combine substantial aortic dilatation, which may weaken their aortic wall, with strong spatio-temporal cross-sectional pressure differences, linked to stronger vortices and potential subsequent extra-dilation. Of course, this is an hypothesis that further specific studies should confirm.

The main limitation of our study is group size. Although the targeted associations were significant despite such small numbers, including more subjects is necessary in order to strengthen conclusions of this preliminary work. In addition, a longitudinal follow-up of the patients is mandatory in future studies using all these innovative 4D flow MRI quantitative indices to evaluate their added value, as compared to conventional geometrical characterization of the aorta in the identification of at-risk patients.

Conclusion

A non-invasive and comprehensive characterization of aortic geometry, blood flow patterns, flow-wall interactions and inner cross-sectional pressure gradients is now rendered possible while using 4D flow MRI. Such evaluation allowed for studying flow-pressure complementarity in healthy aging and for potential identification of patients with dilated ascending aorta concomitant with high cross-sectional pressure gradients, as compared to age-matched healthy individuals. Application to a larger database with longitudinal follow-up may aid in elucidating the usefulness of such interplay in patients with aortic diseases.

List of abbreviations

CMR: Cardiovascular magnetic resonance imaging

4D flow MRI: CMR sequence with velocity encoding in the three directions and full three-dimensional anatomical coverage resolved throughout the cardiac cycle

PC-MRA: phase-contrast MR angiography

AscAo: Ascending aorta

AR: aortic regurgitation

ATAA: Ascending thoracic aortic aneurysm

BSA: Body surface area

SBP: Systolic blood pressure

DBP: Diastolic blood pressure

PP: Pulse pressure

SPGR: spoiled gradient recalled

WSS: wall shear stress

Declarations

A. Ethics approval and consent to participate:

This study conformed to local ethics committee regulations. Ethics committee approval was waived for this study type. Signed informed consent was given by all participants.

B. Consent for publication:

Not applicable.

C. Availability of data and material:

The datasets used and/or analysed during the current study are available from the corresponding author on reasonable request.

D. Fundings

We would like to acknowledge the FRM project ING20150532487 for funding Kevin Bouaou and ESME-Sudria for funding Sophia Houriez--Gombaud-Saintonge as well as the ECOS-SUD project number A15S04 (France-Argentina) exchange grant for funding a fruitful exchange around 4D flow MRI data processing.

E. Acknowledgments

Not applicable.

F. Authors' contributions

All authors contributed significantly to this manuscript.

All authors: manuscript drafting or manuscript revision for important intellectual content

All authors: approval of final version of submitted manuscript

All authors: literature research

K.B., S.H., E.M., G.S., U.G., A.G., EMe., T.D., E.B., D.L., N.K. study concepts/study design or data acquisition or data and statistical analysis or findings interpretation

S.H., T.D., A.D., K.B., I.B., E.J., E.B., N.K., software design for quantification and analysis

G. Competing interests:

The authors declare that they have no competing interests

References

1. Ince H, Nienaber CA. Etiology, pathogenesis and management of thoracic aortic aneurysm. Nat Clin Pract Cardiovasc Med. 2007;4:418–27.

2. ESC Guidelines. 2014 ESC Guidelines on the diagnosis and treatment of aortic diseases: Document covering acute and chronic aortic diseases of the thoracic and abdominal aorta of the adultThe Task Force for the Diagnosis and Treatment of Aortic Diseases of the European Society of Cardiology (ESC). Eur Heart J. 2014;35:2873–926.

3. Pape LA, Tsai TT, Isselbacher EM, Oh JK, O'gara PT, Evangelista A, et al. Aortic diameter >or = 5.5 cm is not a good predictor of type A aortic dissection: observations from the International Registry of Acute Aortic Dissection (IRAD). Circulation. 2007;116:1120–7.

4. Dietenbeck T, Craiem D, Rosenbaum D, Giron A, De Cesare A, Bouaou K, et al. 3D aortic morphology and stiffness in MRI using semi-automated cylindrical active surface provides optimized description of the vascular effects of aging and hypertension. Comput Biol Med. 2018;103:101–8.

5. Callaghan FM, Bannon P, Barin E, Celemajer D, Jeremy R, Figtree G, et al. Age-related changes of shape and flow dynamics in healthy adult aortas: A 4D flow MRI study. J Magn Reson Imaging. 2019;49:90–100.

6. Craiem D, Casciaro ME, Graf S, Chironi G, Simon A, Armentano RL. Effects of aging on thoracic aorta size and shape: A non-contrast CT study. Intl Conf IEEE Eng Med Biol Soc EMBS12. IEEE; 2012. p. 4986--4989.

7. Dyverfeldt P, Bissell M, Barker AJ, Bolger AF, Carlhäll C-J, Ebbers T, et al. 4D flow cardiovascular magnetic resonance consensus statement. J Cardiovasc Magn Reson [Internet]. 2015 [cited 2018 Feb 12];17. Available from: http://jcmr-online.com/content/17/1/72

8. Fatehi Hassanabad A, Burns F, Bristow MS, Lydell C, Howarth AG, Heydari B, et al. Pressure drop mapping using 4D flow MRI in patients with bicuspid aortic valve disease: A novel marker of valvular obstruction. Magn Reson Imaging. 2020;65:175–82.

9. Sigovan M, Hope MD, Dyverfeldt P, Saloner D. Comparison of four-dimensional flow parameters for quantification of flow eccentricity in the ascending aorta. J Magn Reson Imaging. 2011;34:1226–30.

10. Callaghan FM, Grieve SM. Normal patterns of thoracic aortic wall shear stress measured using four-dimensional flow MRI in a large population. Am J Physiol-Heart Circ Physiol. 2018;315:H1174–81.

11. Kauhanen SP, Hedman M, Kariniemi E, Jaakkola P, Vanninen R, Saari P, et al. Aortic dilatation associates with flow displacement and increased circumferential wall shear stress in patients without aortic stenosis: A prospective clinical study. J Magn Reson Imaging. 2019;50:136–45.

12. Spiczak J, Crelier G, Giese D, Kozerke S, Maintz D, Bunck AC. Quantitative Analysis of Vortical Blood Flow in the Thoracic Aorta Using 4D Phase Contrast MRI. Dasi LP, editor. PLOS ONE. 2015;10:e0139025.

13. Bock J, Frydrychowicz A, Lorenz R, Hirtler D, Barker AJ, Johnson KM, et al. In vivo noninvasive 4D pressure difference mapping in the human aorta: Phantom comparison and application in healthy volunteers and patients: Pressure Difference Mapping in the Aorta. Magn Reson Med. 2011;66:1079–88.

14. Bouaou K, Bargiotas I, Dietenbeck T, Bollache E, Soulat G, Craiem D, et al. Analysis of aortic pressure fields from 4D

flow MRI in healthy volunteers: Associations with age and left ventricular remodeling: 4D Flow MRI Aortic Pressure in Aging. J Magn Reson Imaging. 2019;50:982–93.

15. Jeong J, Hussain F. On the identification of a vortex. J Fluid Mech. 1995;285:69.

16. Elbaz MSM, Calkoen EE, Westenberg JJM, Lelieveldt BPF, Roest AAW, Geest RJ. Vortex flow during early and late left ventricular filling in normal subjects: quantitative characterization using retrospectively-gated 4D flow cardiovascular magnetic resonance and three-dimensional vortex core analysis. J Cardiovasc Magn Reson Off J Soc Cardiovasc Magn Reson. 2014;16:78.

17. Potters WV, van Ooij P, Marquering H, vanBavel E, Nederveen AJ. Volumetric arterial wall shear stress calculation based on cine phase contrast MRI. J Magn Reson Imaging JMRI. 2015;41:505–16.

18. Lamata P, Pitcher A, Krittian S, Nordsletten D, Bissell MM, Cassar T, et al. Aortic relative pressure components derived from four-dimensional flow cardiovascular magnetic resonance. Magn Reson Med. 2014;72:1162–9.

19. Donati F, Figueroa CA, Smith NP, Lamata P, Nordsletten DA. Non-invasive pressure difference estimation from PC-MRI using the work-energy equation. Med Image Anal. 2015;26:159–72.

20. Ebbers T, Farnebäck G. Improving computation of cardiovascular relative pressure fields from velocity MRI. J Magn Reson Imaging. 2009;30:54–61.

21. Rengier F, Delles M, Eichhorn J, Azad Y-J, von Tengg-Kobligk H, Ley-Zaporozhan J, et al. Noninvasive 4D pressure difference mapping derived from 4D flow MRI in patients with repaired aortic coarctation: comparison with young healthy volunteers. Int J Cardiovasc Imaging. 2015;31:823–30.

22. Houriez--Gombaud-Saintonge S, Mousseaux E, Bargiotas I, De Cesare A, Dietenbeck T, Bouaou K, et al. Comparison of different methods for the estimation of aortic pulse wave velocity from 4D flow cardiovascular magnetic resonance. J Cardiovasc Magn Reson. 2019;21:75.

23. Soulat G, Gencer U, Kachenoura N, Villemain O, Messas E, Boutouyrie P, et al. Changes in segmental pulse wave velocity of the thoracic aorta with age and left ventricular remodelling. An MRI 4D flow study. J Hypertens. 2020;38:118–26.

24. van Ooij P, Potters WV, Nederveen AJ, Allen BD, Collins J, Carr J, et al. A methodology to detect abnormal relative wall shear stress on the full surface of the thoracic aorta using four-dimensional flow MRI. Magn Reson Med. 2015;73:1216--1227.

25. van Ooij P, Garcia J, Potters WV, Malaisrie SC, Collins JD, Carr JC, et al. Age-related changes in aortic 3D blood flow velocities and wall shear stress: Implications for the identification of altered hemodynamics in patients with aortic valve disease. J Magn Reson Imaging. 2016;43:1239--1249.

26. Ha H, Ziegler M, Welander M, Bjarnegård N, Carlhäll C-J, Lindenberger M, et al. Age-related vascular changes affect turbulence in aortic blood flow. Front Physiol. 2018;9:36.

27. Stalder AF, Russe MF, Frydrychowicz A, Bock J, Hennig J, Markl M. Quantitative 2D and 3D phase contrast MRI: Optimized analysis of blood flow and vessel wall parameters. Magn Reson Med. 2008;60:1218–31.

28. Zimmermann J, Demedts D, Mirzaee H, Ewert P, Stern H, Meierhofer C, et al. Wall shear stress estimation in the aorta: Impact of wall motion, spatiotemporal resolution, and phase noise: Wall Motion Impact on WSS. J Magn Reson Imaging. 2018;48:718–28.

29. Sieren MM, Schultz V, Fujita B, Wegner F, Huellebrand M, Scharfschwerdt M, et al. 4D flow CMR analysis comparing patients with anatomically shaped aortic sinus prostheses, tube prostheses and healthy subjects introducing the wall shear stress gradient: a case control study. J Cardiovasc Magn Reson. 2020;22:59.

30. Ferdian E, Dubowitz DJ, Mauger CA, Wang A, Young AA. WSSNet: Aortic Wall Shear Stress Estimation Using Deep Learning on 4D Flow MRI. Front Cardiovasc Med. 2022;8:769927.

31. Guzzardi DG, Barker AJ, van Ooij P, Malaisrie SC, Puthumana JJ, Belke DD, et al. Valve-Related Hemodynamics Mediate Human Bicuspid Aortopathy. J Am Coll Cardiol. 2015;66:892–900.

32. van Ooij P, Markl M, Collins JD, Carr JC, Rigsby C, Bonow RO, et al. Aortic Valve Stenosis Alters Expression of Regional Aortic Wall Shear Stress: New Insights From a 4-Dimensional Flow Magnetic Resonance Imaging Study of 571 Subjects. J Am Heart Assoc. 2017;6.

33. Bollache E, Guzzardi DG, Sattari S, Olsen KE, Di Martino ES, Malaisrie SC, et al. Aortic valve-mediated wall shear stress is heterogeneous and predicts regional aortic elastic fiber thinning in bicuspid aortic valve-associated aortopathy. J Thorac Cardiovasc Surg. 2018;156:2112-2120.e2.

34. Guala A, Dux-Santoy L, Teixido-Tura G, Ruiz-Muñoz A, Galian-Gay L, Servato ML, et al. Wall Shear Stress Predicts Aortic Dilation in Patients With Bicuspid Aortic Valve. JACC Cardiovasc Imaging. 2022;15:46–56.

35. Rodríguez-Palomares JF, Dux-Santoy L, Guala A, Kale R, Maldonado G, Teixidó-Turà G, et al. Aortic flow patterns and wall shear stress maps by 4D-flow cardiovascular magnetic resonance in the assessment of aortic dilatation in bicuspid aortic valve disease. J Cardiovasc Magn Reson [Internet]. 2018 [cited 2019 Nov 26];20. Available from: https://jcmr-online.biomedcentral.com/articles/10.1186/s12968-018-0451-1

36. Kilner PJ, Yang GZ, Mohiaddin RH, Firmin DN, Longmore DB. Helical and retrograde secondary flow patterns in the aortic arch studied by three-directional magnetic resonance velocity mapping. Circulation. 1993;88:2235–47.

37. Bürk J, Blanke P, Stankovic Z, Barker A, Russe M, Geiger J, et al. Evaluation of 3D blood flow patterns and wall shear stress in the normal and dilated thoracic aorta using flow-sensitive 4D CMR. J Cardiovasc Magn Reson. 2012;14:84.

38. Geiger J, Arnold R, Herzer L, Hirtler D, Stankovic Z, Russe M, et al. Aortic wall shear stress in Marfan syndrome: Aortic WSS in Marfan Syndrome. Magn Reson Med. 2013;70:1137–44.

39. Bensalah MZ, Bollache E, Kachenoura N, Giron A, Cesare AD, Macron L, et al. Geometry is a major determinant of flow reversal in proximal aorta. Am J Physiol - Heart Circ Physiol. 2014;306:H1408–16.

40. Weiss EK, Jarvis K, Maroun A, Malaisrie SC, Mehta CK, McCarthy PM, et al. Systolic reverse flow derived from 4D flow cardiovascular magnetic resonance in bicuspid aortic valve is associated with aortic dilation and aortic valve stenosis: a cross sectional study in 655 subjects. J Cardiovasc Magn Reson. 2023;25:3.

41. Tasu JP, Mousseaux E, Delouche A, Oddou C, Jolivet O, Bittoun J. Estimation of pressure gradients in pulsatile flow from magnetic resonance acceleration measurements. Magn Reson Med. 2000;44:66–72.

42. Meier S, Hennemuth A, Friman O, Bock J, Markl M, Preusser T. Non-invasive 4D blood flow and pressure quantification in central blood vessels via PC-MRI. 2010. p. 903–6.

43. Weigang E, Kari FA, Beyersdorf F, Luehr M, Etz CD, Frydrychowicz A, et al. Flow-sensitive four-dimensional magnetic resonance imaging: flow patterns in ascending aortic aneurysms. Eur J Cardiothorac Surg. 2008;34:11–6.

Tables

Table 1. Subjects characteristics, and MRI measurements in the ascending aorta.

Parameter	Young controls	Elderly controls	ATAA patients
n (men/women)	13 (9/4)	17 (12/5)	17 (12/5)
Age (years)	33.5±11.1	59.7±13.3^{+}	64.7±14.3
BSA (m^2)	1.7±0.20	1.8±0.20	1.9±0.34
SBP (mmHg)	111.6±13.4	116.1±11.0	117.8±16.3
DBP (mmHg)	79.9±9.1	81.8±5.4	80.6±9.6
D_{MAX} (mm)	27.8±2.4	31.4±3.3^{+}	42.9±4.9*
iD_{MAX} (mm/m^2)	16.2±1.5	17.4±2.2	23.1±4.7*
Vol_{AscAo}(mL)	26.4±7.5	36.9±10.9^{+}	95.13±40.19*
$iVol_{AscAo}$(mL/m^2)	15.2±3.6	20.2±5.7^{+}	49.4±17.6*
WSS_{MAX} (Pa)	0.87±0.15	0.69±0.20^{+}	0.54±0.15*
V_{MAX} (s^{-1})	121.7±64.6	95.6±52.6	67.2±46.1*
V_{ECC}	0.24±0.05	0.25±0.03	0.19±0.09*

V_{FWHM} (ms)	334.1±120.9	440.8±118.0^{+}	631.1±197.4*
ΔP_S (mmHg)	1.7±0.6	1.6±0.6	1.6±0.7
ΔD_{PS} (mm)	13.7±2.6	15.7±3.2^{+}	19.3±4.3*
ΔP_T (mmHg)	2.0±1.1	1.7±0.5	1.5±0.5
ΔT_{PT} (ms)	268.5±65.6	213.1±71.8	132.8±58.1*

BSA: body surface area, SBP/DBP: systolic/diastolic blood pressure, AscAo: ascending aorta, D_{MAX}/iD_{MAX}: non-indexed/indexed maximal AscAo diameter, Vol_{AscAo}/$iVol_{AscAo}$: non-indexed/indexed AscAo volume, WSS_{MAX}: AscAo maximal wall shear stress, V_{MAX}: AscAo maximal vorticity magnitude, V_{ECC}: AscAo vortex eccentricity, V_{FWHM}: AscAo vortex duration, ΔP_S: cross-sectional maximal pressure difference through the AscAo, ΔD_{P_S}: distance between pressure extrema within the AscAo, ΔP_T: difference in magnitude between systolic and diastolic relative pressure peaks within the AscAo, ΔT_{P_T}: duration between systolic and diastolic pressure peaks within the AscAo. + indicates significance of comparisons between elderly and young healthy subjects, * indicates significance of comparisons between ATAA patients and elderly controls.

Table 2. **Associations between ascending aorta hemodynamic and morphological indices (whole group, n=47)**.

	D_{MAX} (r, p)	**iD_{MAX} (r, p)**	**Vol_{AscAo} (r, p)**	**$iVol_{AscAo}$ (r, p)**
WSS_{MAX}	(-0.66, <0.001)*	(-0.49, <0.001)*	(-0.60, <0.001)*	(-0.63, <0.001)*
V_{MAX}	(-0.30, 0.040)	ns.	ns.	(-0.29, 0.048)
V_{ECC}	(-0.44, 0.002)*	(-0.29, 0.045)	(-0.51, <0.001)*	(-0.51, <0.001)*

V_{FWHM}	(0.56, <0.001)*	(0.48, <0.001)*	(0.47, <0.001)	(0.53, <0.001)
ΔP_S	ns.	ns.	ns.	ns.
ΔD_{PS}	(0.64, <0.001)*	(0.37, 0.010)	(0.56, <0.001)	(0.54, <0.001)*
ΔP_T	ns.	ns.	ns.	ns.
ΔT_{PT}	(-0.69, <0.001)*	(-0.52, <0.001)*	(-0.62, <0.001)*	(-0.63, <0.001)*

D_{MAX}/iD_{MAX}: non-indexed/indexed maximal AscAo diameter, Vol_{AscAo}/$iVol_{AscAo}$: non-indexed/indexed AscAo volume, WSS_{MAX}: AscAo maximal wall shear stress, V_{MAX}: AscAo maximal vorticity magnitude, V_{ECC}: AscAo vortex eccentricity, V_{FWHM}: AscAo vortex duration, ΔP_S: cross-sectional maximal pressure difference through the AscAo, ΔD_{PS}: distance between pressure extrema within the AscAo, ΔP_T: difference in magnitude between systolic and diastolic relative pressure peaks within the AscAo, ΔT_{P_T}: duration between systolic and diastolic pressure peaks within the AscAo. Correlation coefficient and the corresponding p value (r, p) are provided for all the studied associations on the entire study group. *remained significant after adjustment for age and systolic blood pressure ($p<0.05$). ns.: non-significant results

Table 3. **Associations between pressure and flow in healthy subjects**.

	ΔP_S (r, p)	**ΔP_T (r, p)**
WSS_{MAX}	(0.59 , <0.001)*	(0.40 , 0.03)
V_{MAX}	(0.55 , 0.002)*	ns.
V_{ECC}	ns.	(-0.40, 0.03)
V_{FWHM}	(-0.40, 0.03)	ns.

AscAo: ascending aorta, WSS_{MAX}: AscAo maximal wall shear stress, V_{MAX}: AscAo maximal vorticity

magnitude, V_{ECC}: AscAo vortex eccentricity, V_{FWHM}: AscAo vortex duration, ΔP_S: cross-sectional maximal pressure difference through the AscAo, ΔP_T: difference in magnitude between systolic and diastolic relative pressure peaks within the AscAo. Correlation coefficient and the corresponding p value (r, p) are provided for studied associations on all healthy controls (30 subjects, 9 women, 48.3±18.0 years). * remained significant after adjustment for age, systolic blood pressure and iD_{MAX} ($p<0.05$). ns. non-significant results

Figure Legends

Figure 1. Aortic 4D flow MRI data processing pipeline.

Upper Panel: 4D flow MRI modulus and velocity components images and aortic segmentation as well as aortic slicing. Bottom Panel: estimation of relative 3D pressure map using iterative Poisson equation and definition of temporal and spatial changes in pressure amplitude (ΔP_T, ΔP_S) as well as temporal and spatial distance between pressure extrema in the ascending aorta (ΔT_{PT}, ΔD_{PS}); estimation of wall shear stress map and definition of the spatio-temporal WSS peak within the ascending aorta (WSS_{MAX}); estimation of vorticity using the λ_2-method and definition of the vortex eccentricity (V_{ECC}), maximal amplitude (V_{MAX}) and duration (V_{FWHM}) within the ascending aorta.

Figure 2: Ascending aorta time-resolved cross-sectional maximal pressure changes.

Individual curves of maximal pressure changes within each ascending aorta cross-sectional slice (grey) and the average curve over all slices (red).

Figure 3: **Aortic 4D flow MRI-derived velocity, relative pressure, WSS and vorticity.** Examples of quantitative hemodynamic maps for a young healthy volunteer (top) and a patient with a dilated ascending aorta (bottom), along with mean (solid lines) and standard deviation (shades) for time-

resoled velocity, WSS, vorticity and relative pressure curves in the ascending aorta of young healthy subjects (grey), elderly healthy subjects (yellow) and ATAA patients (blue). Time curves were rescaled between 0 and 1000 ms for all patients before averaging them and the averaged curve was then truncated at 700 ms.

Figure 4: **Pressure and flow associations in healthy volunteers.**

Associations between cross-sectional spatial pressure difference (ΔPs) and flow indices within the ascending aorta of healthy subjects (young controls in grey and healthy elderly controls matched to ATAA patients in orange): WSS_{MAX} (A) as well as maximal vorticity magnitude V_{MAX} (B).

Figure 5: **Examples of extreme values of ascending aorta cross sectional pressure changes**

High (left) and low (right) ascending aorta cross sectional pressure changes along with the corresponding velocity, WSS and vorticity curves throughout the cardiac cycle.

Figure 6: **Pressure and flow associations in aortic dilation.**

Patients with aortic dilation (blue) are superimposed to linear regression dot plots obtained on young (grey) and elderly (orange) healthy subjects for associations between AscAo pressure cross-sectional spatial difference and WSS (A) and between AscAo pressure cross-sectional spatial difference and vorticity magnitude (B). Patients with elevated spatial pressure differences despite pronounced AscAo dilation are highlighted with red circles.

Figures

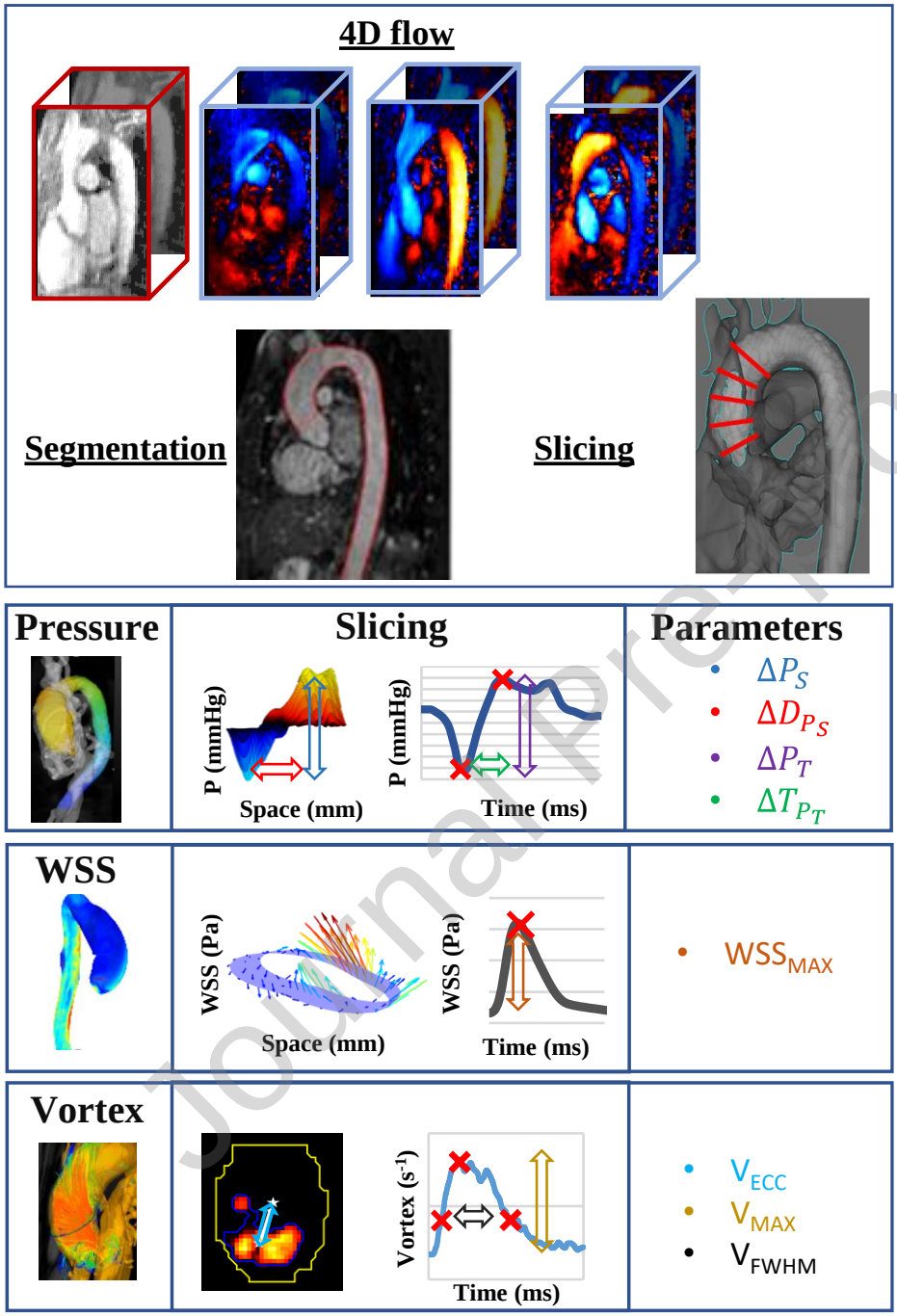

Figure 1. Aortic 4D flow MRI data processing pipeline.

Upper Panel: 4D flow MRI modulus and velocity components images and aortic segmentation as well as aortic cross-sectional slicing. Bottom Panel: estimation of relative 3D pressure map using iterative

Poisson equation and definition of temporal and spatial changes in pressure amplitude (ΔP_T, ΔP_S) as well as temporal and spatial distance between pressure extrema in the ascending aorta (ΔT_{PT}, ΔD_{PS}); estimation of wall shear stress map and definition of the spatio-temporal WSS peak within the ascending aorta (WSS_{MAX}); estimation of vorticity using the λ_2-method and definition of the vortex eccentricity (V_{ECC}), maximal amplitude (V_{MAX}) and duration (V_{FWHM}) within the ascending aorta.

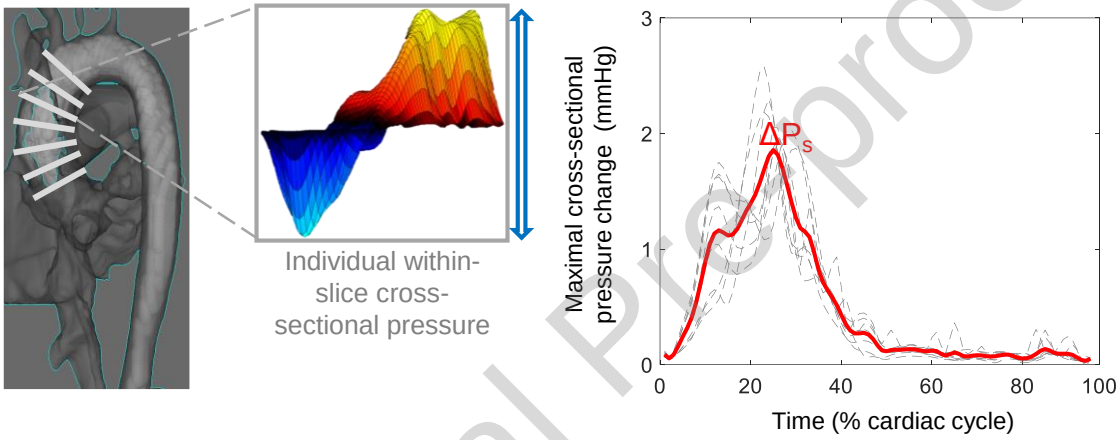

Figure 2: Ascending aorta time-resolved cross-sectional maximal pressure changes.

Individual curves of maximal pressure changes within each ascending aorta cross-sectional slice (grey) and the average curve over all slices (red).

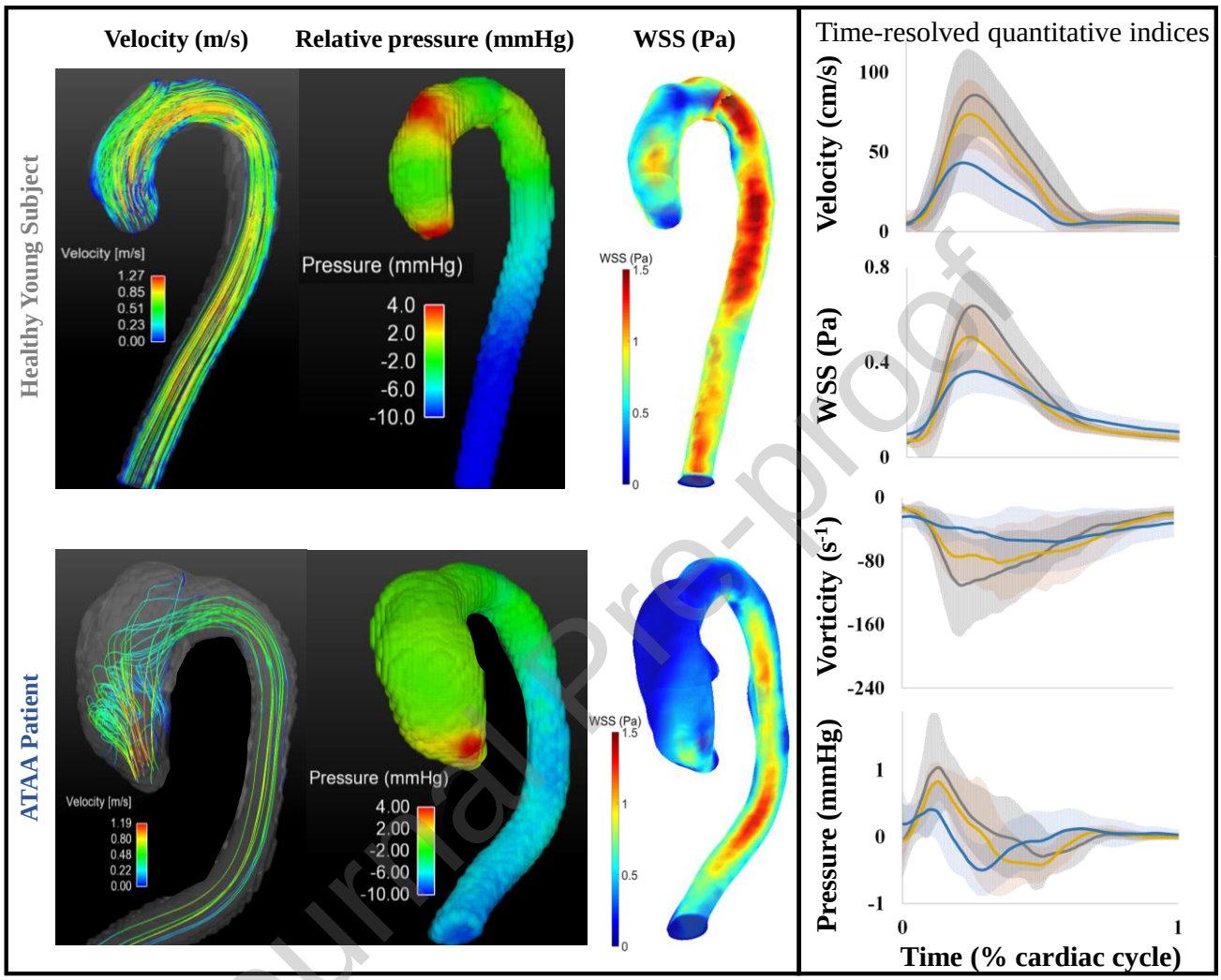

Figure 3: **Aortic 4D flow MRI-derived velocity, relative pressure, WSS and vorticity.** Examples of quantitative hemodynamic maps for a young healthy volunteer (top) and a patient with a dilated ascending aorta (bottom), along with mean (solid lines) and standard deviation (shades) for time-resoled velocity, WSS, vorticity and relative pressure curves in the ascending aorta of young healthy subjects (grey), elderly healthy subjects (yellow) and ATAA patients (blue). Time curves were rescaled between 0 and 1000 ms for all patients before averaging them and the averaged curve was then truncated at 700 ms.

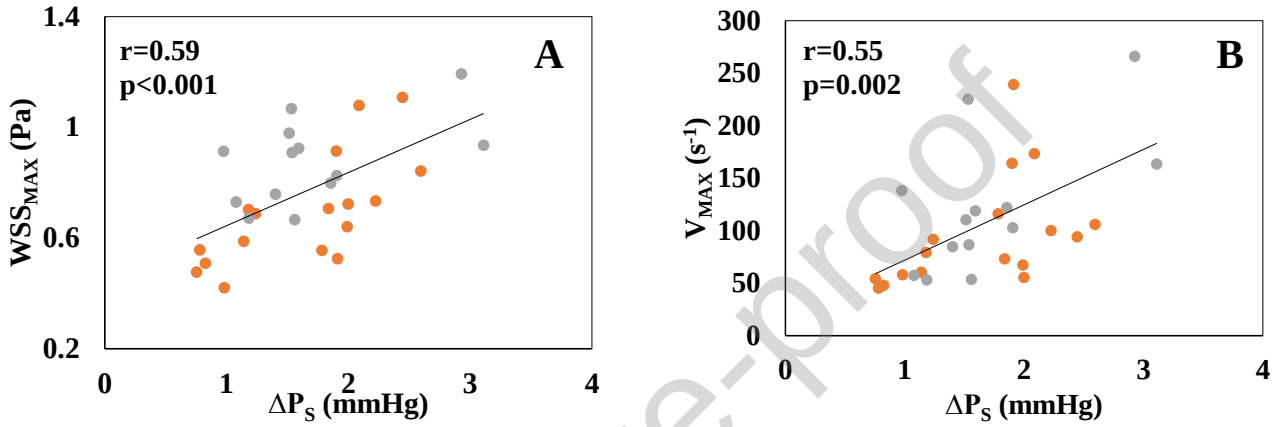

Figure 4: **Pressure and flow associations in healthy volunteers.**

Associations between cross-sectional spatial pressure difference (ΔPs) and flow indices within the ascending aorta of healthy subjects (young controls in grey and healthy elderly controls matched to ATAA patients in orange): WSS_{MAX} (A) as well as maximal vorticity magnitude V_{MAX} (B).

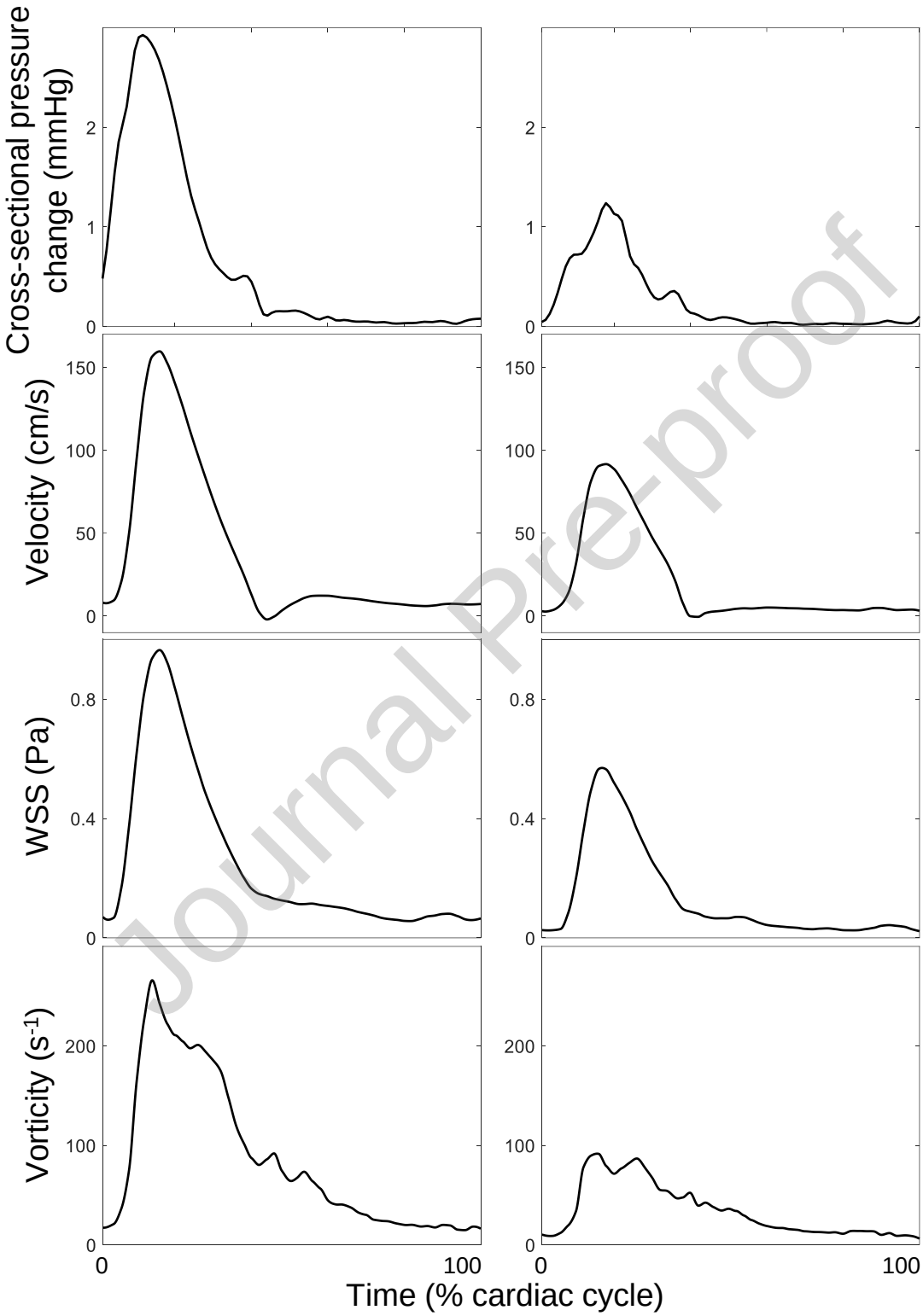

Figure 5: **Examples of extreme values of ascending aorta cross sectional pressure changes**

High (left) and low (right) ascending aorta cross sectional pressure changes along with the corresponding velocity, WSS and vorticity curves throughout the cardiac cycle.

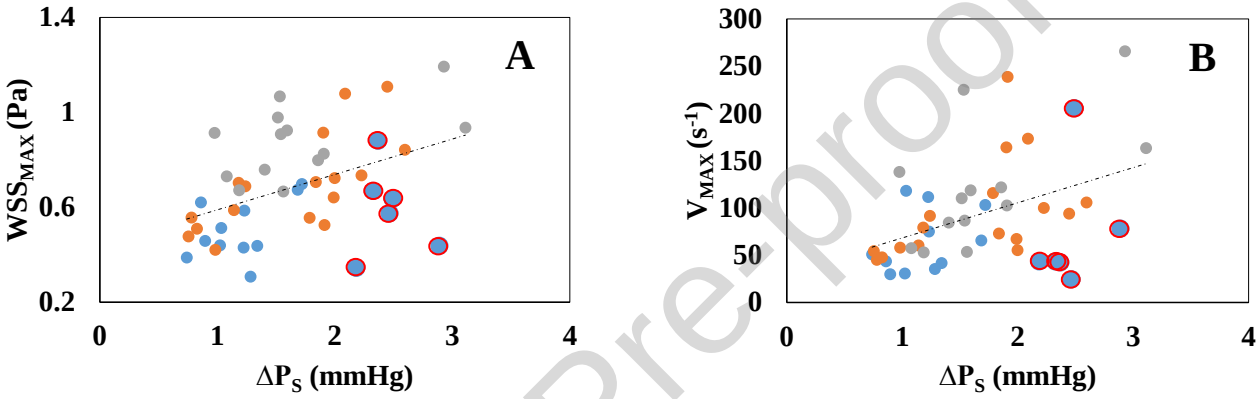

Figure 6: **Pressure and flow associations in aortic dilation.**

Patients with aortic dilation (blue) are superimposed to linear regression dot plots obtained on young (grey) and elderly (orange) healthy subjects for associations between AscAo pressure cross-sectional spatial difference and WSS (A) and between AscAo pressure cross-sectional spatial difference and vorticity magnitude (B). Patients with elevated spatial pressure differences despite pronounced AscAo dilation are highlighted with red circles.

Declaration of Competing Interest

The authors declare the following financial interests/personal relationships which may be considered as potential competing interests Nadjia Kachenoura reports financial support was provided by Fondation pour la recherche Médicale. Sophia Houriez–Gombaud-Saintonge reports a relationship with ESME Sudria that includes: employment. Nadjia Kachenoura reports a relationship with ECOS SUD that includes: funding grants. If there are other authors, they declare that they have no known competing financial interests or personal relationships that could have appeared to influence the work reported in this paper.